

Mathematical and Intelligent Modeling of Electropneumatic Servo Actuator Systems

Hazem I. Ali, Samsul Bahari B Mohd Noor, S.M. Bashi, Mohammad Hamiruce Marhaban

Department of Electrical & Electronic Engineering, Faculty of Engineering, University Putra
Malaysia, Malaysia

Abstract: The pneumatic actuator represents the main force control operator in many industrial applications, where its static and dynamic characteristics play an important role in the overall behavior of the control system. Therefore, obtaining of accurate approach for modeling the pneumatic actuator is of prime interest to control system designers. In this paper a different methodologies for deriving and simulating the model of the pneumatic servo actuators controlled with proportional valves are presented. The model includes cylinder dynamics, payload motion, friction and valve characteristics.

Key words: Nonlinear System, Pneumatic actuators, Modeling, Friction modeling.

INTRODUCTION

Pneumatic actuators are widely employed in position and speed control applications when cheap, clean, simple, and safe operating conditions are required. In recent years, low cost microprocessors and pneumatic components became available in the market, which made it possible to adopt more sophisticated control strategies in pneumatic system control (Jihong *et al.*, 2007). Also the pneumatic cylinders can offer a better alternative to electrical or hydraulic actuators for certain types of applications and the pneumatic actuators provide the previously enumerated qualities at low cost. They are also suitable for clean environments and safer and easier to work with. However, position and force control of these actuators in applications that require high bandwidth is some how difficult, because of compressibility of air and highly nonlinear flow through pneumatic system components (Edmod and Yildirim, 2001). A typical pneumatic system includes a force element (pneumatic cylinder), a command device (valve), connecting tubes, and piston, pressure and force sensors. The external load consists of the mass of external mechanical elements connected to the piston and perhaps a force produced by environmental interaction. A schematic diagram of the pneumatic actuator system is shown in Figure 1.

The final decision on the best type and design configuration for pneumatic actuator can be made only in relation to the requirements of a particular application. The pneumatic actuator has most often been of the piston cylinder type because of its low cost and simplicity (Tablin and Gregory, 1963). The pneumatic power is converted to straight line reciprocating and rotary motions by pneumatic cylinders and pneumatic motors. The pneumatic position servo systems are used in numerous applications because of their ability to position loads with high dynamic response and to augment the force required moving the loads. Pneumatic systems are also very reliable (Clements and Len., 1985).

Pneumatic systems have many attributes that make them attractive for use in difficult environments. The important attributes are: (i) gases are not subjected to the temperature limitations of hydraulic fluids; (ii) the actuator exhaust gases need not be collected, so fluid return lines are unnecessary and long term storage is not a problem because pneumatic systems are virtually dry and no organic materials need be used. In addition, the pneumatic actuator has a lower specific weight and a higher power rate (torque-squared to inertia ratio) than an equivalent electromechanical actuator. In some cases, a pneumatic system may provide a significant weight advantage. In short duration missile applications, the weight of a self-contained solid propellant pneumatic servo may be half that of an equivalent self contained hydraulic system. Also the pneumatic actuators have many merits such as easy maintenance and handling, relatively simple technology and low cost, clean, safe and easy to installed (Tablin and Gregory, 1963).

In this paper a different methodologies for deriving the mathematical model of pneumatic servo actuator are reviewed. The model includes cylinder dynamics, payload motion, friction and valve characteristics.

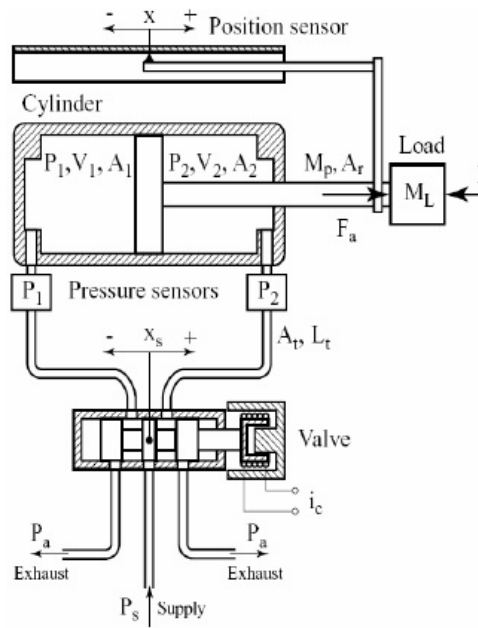


Fig. 1: Schematic diagram of double acting pneumatic actuator system.

Nonlinear Mathematical Modeling:

Several approaches have been proposed for modeling the pneumatic actuators. One of the widely used methods for finding the mathematical model of the pneumatic actuator is a theoretical analysis. The analysis of pneumatic actuators requires a combination of thermodynamics, fluid dynamics and the dynamics of the motion. For constructing a mathematical model, three major considerations must be involved: 1) the determination of the mass flow rates through the valve. 2) the determination of the pressure, volume and temperature of the air in cylinder. 3) the determination of the dynamics of the load (French and Cox, 1988).

Valve Mass Flow Rate Model:

The pneumatic valve is a critical component of the actuator system. It is the command element, and should be able to provide fast and precisely controlled airflows in and out of the actuator chambers. There are many available designs for pneumatic valves, which differ by geometry of the active orifice, type of flow regulating element, number of paths and ports, and type of actuating etc. One of the common used valves is the pneumatic proportional spool valve. The modeling of this valve involves two aspects: the dynamics of the valve spool, and the mass flow through the valve's orifice. The equation of motion for the valve spool can be written as (Edmond and Yildirim, 2001).

$$M_s \ddot{x}_s + C_s \dot{x}_s + F_f + 2k_s x_s = K_{fc} i_c \tag{1}$$

where M_s is the spool and coil assembly mass, x_s is the spool displacement, c_s is the viscous friction coefficient, F_f is the friction force and can be neglected, K_s is the spool springs constant, K_{fc} is the coil force coefficient, and i_c is the coil current. Figure 2 shows the valve spool dynamic equilibrium (Edmod and Yildirim, 2001).

The pressure drop across the valve orifice is usually large, and the flow has to be treated as compressible and turbulent. If the upstream to downstream pressure ratio is larger than a critical value (P_{cr}), the flow will attain sonic velocity (choked flow) and will depend linearly on the upstream pressure. If the pressure ratio is smaller than P_{cr} the mass flow depends nonlinearly on both pressures. The standard equation for the mass flow through an orifice of area A_v is (Edmod and Yildirim, 2001).

$$\dot{m}_v = C_f A_v C_1 \frac{P_u}{\sqrt{T}} \dots \frac{P_d}{P_u} \leq P_{cr}$$

$$\dot{m}_v = C_f A_v C_2 \frac{P_u}{\sqrt{T}} \left(\frac{P_d}{P_u} \right)^{1/k} \sqrt{1 - \left(\frac{P_d}{P_u} \right)^{(k-1)/k}} \dots \frac{P_d}{P_u} > P_{cr} \tag{2}$$

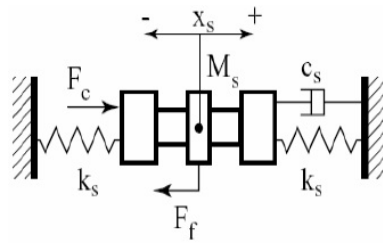


Fig. 2: Valve spool dynamic equilibrium.

where \dot{m}_v is the mass flow through valve orifice, C_f is a nondimensional discharge coefficient, k is the specific heat ratio, R is the universal gas constant, T is the temperature, P_u , P_d are the upstream and downstream pressures, and

$$C_1 = \sqrt{\frac{k}{R} \left(\frac{2}{k+1} \right)^{\frac{k+1}{k-1}}}; C_2 = \sqrt{\frac{2k}{R(k-1)}}; P_{cr} = \left(\frac{2}{k+1} \right)^{\frac{k}{k-1}} \quad (3)$$

are constants for a given fluid. For air ($k=1.4$), so $C_1 = 0.040418$, $C_2 = 0.156174$, and $P_{cr} = 0.528$ (Han *et al.*, 2002; Xuesong and Guangzheng, 2003; Shu and Gary, 2005; Xue *et al.*, 2007; Zhihong and Gary, 2008).

A new modeling approach to develop the nonlinear system model using a combination of mechanistic and empirical method is presented in (Zhihong and Gary, 2008). To model the valve flow rates, the use of bipolynomial function was used to produce a more accurate solution than prior approaches. The dynamic model of the system was given as follows (Zhihong and Gary, 2008).

$$\dot{m}_{11} = \lambda_1(u_1, P_1), \dot{m}_{22} = \lambda_2(u_2, P_1), \dot{m}_{33} = \lambda_3(u_3, P_2), \dot{m}_{44} = \lambda_4(u_4, P_2), \dot{m}_1 = \dot{m}_{11} - \dot{m}_{22}, \dot{m}_2 = \dot{m}_{33} - \dot{m}_{44} \quad (4)$$

where $\dot{m}_{11} - \dot{m}_{22}$, $\dot{m}_2 = \dot{m}_{33}$ and \dot{m}_{44} are mass flow rates through the four valves shown in Figure 3; \dot{m}_{11} and \dot{m}_2 are the mass flow rates of the two chambers; u_1 , u_2 , u_3 , and u_4 are valve input voltages; λ_1 to λ_4 are nonlinear functions modeling the mass flow rate; P_1 , P_2 are the pressures of two chambers. The mass flow rate model of the proportional valve is a key part of the system model. The proportional valve that was used in (Zhihong and Gary, 2008). consists of a spring-loaded flat plate covering a spray nozzle, and an electro-magnet for moving the plate. Its structure is different from the traditional spool servo valve so it was necessary to derive a new mass flow rate model.

The mass flow rates at different pressures and valve input voltages were first estimated from the pressure versus time responses obtained from step inputs in valve voltage and a fixed piston position. The fit of several functions was evaluated in (Zhihong and Gary, 2008). and found that a 2nd order bipolynomial function provided the best fit. The equation is:

$$\dot{m}_{11} = \lambda_1(u_1, P_1), a_1 + b_1 P_1 + c_1 P_1^2 + d_1 u_1 P_1 + f_1 u_1 P_1^2 + g_1 u_1^2 + h_1 u_1^2 P_1 + i_1 u_1^2 P_1^2 \quad (5)$$

where $a_1, b_1, d_1, e_1, f_1, g_1, h_1$ and i_1 are the coefficients. The coefficients for all equations were obtained using nonlinear least squares (Zhihong and Gary, 2008).

Actuator Cylinder Model:

The dynamic of the pneumatic actuator is described using equilibrium, continuity and energy equations, according to the lumped parameters model of the system. In the first case the equilibrium and the air mass continuity equations are chosen to describe the actuator dynamics. The fluid behavior is evaluated separately in the two chambers, with a variable volume, by means of the continuity equations, assuming that the air transformation follows a generic polytropic. The chambers pressures and the system kinetic variables are related by the equilibrium equation of the mobile elements. The feedbacks on the continuity equations are the piston speed and displacement, which determines the chambers volumes. The continuity equation of air is (Sorli *et al.*, 1999).

$$\dot{m}_j = \rho_{j\dot{i}} \left(\frac{P_j}{P_{j\dot{i}}} \right)^{\frac{1}{n}} = \frac{P_{j\dot{i}}}{RT_{j\dot{i}}} \left(\frac{P_j}{P_{j\dot{i}}} \right)^{\frac{1}{n}} \tag{6}$$

where ρ is the air density, V is the volume of the chamber and j represents the chamber (where $j = 1, 2$). Considering a polytropic transformation with index n which denotes the polytropic index of expansion or compression and assuming that the air can be considered a perfect gas, one has (Sorli *et al.*, 1999).

$$\rho_j = \rho_{j\dot{i}} \left(\frac{P_j}{P_{j\dot{i}}} \right)^{\frac{1}{n}} = \frac{P_{j\dot{i}}}{RT_{j\dot{i}}} \left(\frac{P_j}{P_{j\dot{i}}} \right)^{\frac{1}{n}} \tag{7}$$

where the subscript i identifies initial conditions. The volume V_j is a function of the stroke, of the dead volume and of the piston displacement.

$$V_j = A_j (x_0 \pm x) + V_{mj} = A_j (x_0 \pm x + x_{mj}) \tag{8}$$

where A_j is the piston area, x_0 is the half stroke displacement, x is the piston displacement, x_m is the dead displacement, V_m is the dead volume. The positive sign should be considered when $j=1$ and the negative one when $j=2$. By substituting equations (7) and (8) in (6), the following expression is obtained (Sorli *et al.*, 1999).

$$\dot{m}_1 = A_j (x_0 \pm x \pm x_{mj}) \frac{1}{nRT_{j\dot{i}}} \left(\frac{P_j}{P_{j\dot{i}}} \right)^{\frac{1}{n}-1} \frac{dP_j}{dt} \pm \frac{P_{j\dot{i}}}{RT_{j\dot{i}}} \left(\frac{P_j}{P_{j\dot{i}}} \right)^{\frac{1}{n}} A_j \frac{dx}{dt} \tag{9}$$

and the pressure rate is:

$$\frac{dP_j}{dt} = \frac{nRT_{j\dot{i}}}{A_j (x_0 \pm x + x_{mj}) \left(\frac{P_j}{P_{j\dot{i}}} \right)^{\frac{1}{n}-1}} \dot{m}_j \pm \frac{nP_j}{(x_0 \pm x + x_{mj})} \frac{dx}{dt} \tag{10}$$

The estimation of the value of n is quite complex and mostly it could not be constant with the stroke and it could depend on the working conditions. Generally isothermal transformations can be assumed for sufficiently slow cycles, while with high working frequencies the heat flow between the system and the extern can be neglected, and then the transformation follows an adiabatic process (Sorli *et al.*, 1999).

By assuming that there is no heat transfer during the running time, i.e. the process is adiabatic and applying the first law of thermodynamics and the ideal gas law to the two chambers, the dynamic equations of the cylinder chambers will be:

$$KRT\dot{m}_1 = (KA_1\dot{x})P_1 + (A_1x + V_{1o})\dot{P}_1 \tag{11}$$

$$KRT\dot{m}_2 = (KA_2\dot{x})P_2 + [A_2(L - x) + V_{2o}] \dot{P}_2 \tag{12}$$

where A_1 and A_2 are the cross-sectional area of the two chambers, V_{1o} and V_{2o} are the dead volumes (including tubes and connectors) of the two chambers; K is the ratio of specific heats of air; L is the stroke length (Sorli, *et al.*, 1999). Similar equations of cylinder chambers are presented in (Xuesong and Guangzheng, 2003; Zhihong and Gary, 2008; Nieto, *et al.*, 2008 and Chen *et al.*, 2003).

The most general model for a volume of gas consists of three equations: an equation of ideal gas law, the conservation of mass (continuity) equation, and the energy equation. Assuming that (i) the gas is perfect, (ii) the pressures and temperature within the chamber are homogeneous, and (iii) kinetic and potential energy terms are negligible, these equations can be written for each chamber (Edmod and Yildirim, 2001; Djordje and Novak, 2008). The energy equation is:

$$q_{in} - q_{out} + kC_v (\dot{m}_{in}T_{in} - \dot{m}_{out}T) - \dot{W} = \dot{U} \tag{13}$$

where q_{in} and q_{out} are the heat transfer terms, C_v is the specific heat at constant volume, $\dot{m}_{in}, \dot{m}_{out}$ are the mass flows entering and leaving the chamber, T_{in} is the temperature of the incoming gas flow, \dot{W} is the rate of change in the work, and \dot{U} is the change of internal energy. The total change in internal energy \dot{W} is:

$$\dot{U} = \frac{d}{dt}(C_v \dot{m} T) = \frac{1}{k-1} \frac{d}{dt}(PV) = \frac{1}{k-1}(V\dot{P} + P\dot{V}) \tag{14}$$

in which the ideal gas relation was used, $C_v = R/(k - 1)$.

By substituting $\dot{W} = P\dot{V}$, equation (14) into (13), assuming the incoming flow is already at the temperature of the gas in the chamber considered for analysis, the process is considered to be adiabatic ($q_{in} - q_{out} = 0$) and applying the ideal gas law, the time derivative of the chamber pressure is:

$$\dot{P} = k \frac{RT}{V} (\dot{m}_{in} - \dot{m}_{out}) - k \frac{P}{V} \dot{V} \tag{15}$$

If the process is considered to be isothermal ($T = \text{constant}$), then the change in internal energy, energy and the rate of change in pressure equations are:

$$\dot{U} = C_v \dot{m} T \tag{16}$$

$$q_{in} - q_{out} = P\dot{V} - \frac{P}{\rho} (\dot{m}_{in} - \dot{m}_{out}) \tag{17}$$

$$\dot{P} = \frac{RT}{V} (\dot{m}_{in} - \dot{m}_{out}) - \frac{P}{V} \dot{V} \tag{18}$$

A comparison of equation (15) and (18) shows that the only difference is the specific heat ratio term k . Thus, both equations can be written as:

$$\dot{P} = \frac{RT}{V} (\alpha_{in} \dot{m}_{in} - \alpha_{out} \dot{m}_{out}) - \alpha \frac{P}{V} \dot{V} \tag{19}$$

with α , α_{in} and α_{out} taking values between 1 and k , depending on the actual heat transfer during the process.

Choosing the origin of piston displacement at the middle of the stroke, the volume of each chamber can be expressed as:

$$V_j = V_{\emptyset} + A_j \left(\frac{1}{2} L \pm x \right) \tag{20}$$

Substituting equation (20) into (19), the time derivative for the pressure in the pneumatic cylinder chambers becomes:

$$\dot{P}_j = \frac{RT}{V_{\emptyset} + A_j \left(\frac{1}{2} L \pm x \right)} (\alpha_{in} \dot{m}_{in} - \alpha_{out} \dot{m}_{out}) - \alpha \frac{PA_j}{V_{\emptyset} + A_j \left(\frac{1}{2} L \pm x \right)} \dot{x} \tag{21}$$

In this above form the pressure dynamics equation accounts for the different heat transfer characteristics of the charging and discharging process, air compression or expansion due to piston movement, the difference in effective area on the opposite sides of the piston, and the inactive volume at the end of stroke and the admission ports (Edmod and Yildirim, 2001).

Motion Dynamic Model and Friction:

The dynamic equilibrium of motion for the piston-rod-load assembly can be expressed as:

$$(M + M_p) \ddot{x} + F_f + F_d = P_1 A_1 - P_2 A_2 - P_a A_r \tag{22}$$

where M is the external load mass, M_p is the piston and rod assembly mass, x is the piston position, F_f is the friction force, F_d is the external force, P_a is the absolute ambient pressure, and A_r is the rod cross sectional area (Edmod and Yildirim, 2001; Gary and Shu 2007).

In order to compensate friction and achieve precise position control, an accurate and feasible friction model needs to be chosen first. Although friction occurs in almost all mechanical systems, there is no universal friction model that can be used for any system. For different systems and control objectives, different friction models are adopted to ease the task. A simple Gaussian exponential static friction model can be represented in equation (23) as a function of instantaneous sliding velocity \dot{x} , which captures three basic frictions: coulomb, viscous and Stribeck friction (Armstrong and Wit, 1996).

$$F_f = F[\dot{x}] = F_c \operatorname{sgn}[\dot{x}] + F_s e^{-|\dot{x}/v_s|} \operatorname{sgn}(\dot{x}) + F_v \dot{x} \tag{23}$$

where F_c is the coulomb friction, F_s is the magnitude of the Stribeck friction, which is the excess of static friction over coulomb friction, F_v is the viscous friction and v_s is the characteristic velocity of the Stribeck friction. By choosing different parameters, different friction models can be realized.

Linear Mathematical Modeling:

The nonlinear equation (2) that governs the mass flow rate of air through the control valve orifice can be linearized if the valve operates within its mechanical operating range (Mark and Nariman, 2006). Equation (2) can be linearized using a Taylor series expansion about operating point. Neglecting the second and higher order terms as well as any control valve leakages, the mass flows into each actuator chamber are written as:

$$\dot{m}_1 = C_{f1}x_s - C_{p1}P_1 \tag{24}$$

$$\dot{m}_2 = C_{f2}x_s - C_{p2}P_2$$

where C_{fi} and C_{pi} are known as the valve flow gain and flow pressure coefficient, respectively. Their specific values depend upon operating point pressures, P_{1o} and P_{2o} as well as the operating point value of valve spool displacement, x_{so} (Mark and Nariman, 2006). By substituting equation (24) in equations (11) and (12) or (21) and then using equation (22) with taking a viscous friction only, the linear pneumatic actuator model is (Mark and Nariman, 2006).

$$x(s) = G(s)U(s) - G_d(s)F_d(s) \tag{25}$$

$$G(s) = \frac{\gamma RTk_v A \{ C_{f1}(\gamma RTC_{p2} + V_{20}s) + C_{f2}(\gamma RTC_{p1} + V_{10}) \}}{(\tau_v s + 1)D(s)} \tag{26}$$

$$G_d(s) = \frac{(\gamma RTC_{p1} + V_{10})(\gamma RTC_{p2} + V_{20}s)}{D(s)} \tag{27}$$

$$D(s) = s(Ms + F)(\gamma RTC_{p1} + V_{10})(\gamma RTC_{p2} + V_{20}s) + \alpha \gamma A^3 s[\gamma RT(P_{10}C_{p2} + P_{20}C_{p1}) + (P_{10}V_{20} + P_{20}V_{10})s] \tag{28}$$

where K_v is the valve gain, τ_v is the valve time constant, V_{1o} , V_{2o} are volume operating points.

Intelligent Modeling:

It is known that the neural network has learning ability and is a good choice for modeling dynamic and complex process. Levenberg-Marquardt method as the training algorithm of multilayered feedforward neural network, and builds a neural network model for the pneumatic system was adopted in (Marumo and Tokhi, 2004). The conventional digital controller was designed based on a linear model. So an ARX (auto-regressive with external input) model was derived from the weights of the trained neural network. A third order ARX model was derived from the fixed weights of the trained neural network.

The structure of a two-layered feed forward neural network is shown in Figure (4). For the ease of the controller design, linear activation functions are chosen for the hidden layer of the neural network.

The goal of a neural network model is to determine its weights to minimize the following objective function:

$$V_N(\theta, Z^N) = \frac{1}{2N} \sum_{t=1}^N [y(t) - \hat{y}(t \setminus \theta)]^2 = \frac{1}{2N} \sum_{t=1}^N \varepsilon^2(t, \theta) \tag{29}$$

where θ contains all adjustable neural network weights $\{W_j, w_{ji}\}$, Z^N is the dataset consisting of the plant output $y(t)$ and the neural network output $\hat{y}(t)$. To train the neural network the Levenberg-Marquardt method was used for training by taking the following form:

$$\theta^{(i+1)} = \theta^{(i)} + f^{(i)}$$

$$[R(\theta^{(i)}) + \lambda^{(i)} I] f^{(i)} + G(\theta^{(i)}) \tag{30}$$

where $\theta^{(i)}$ specifies the i th iterate; $f^{(i)}$ is the search direction; $\lambda^{(i)}$ is an adjustable parameter; $G(\theta^{(i)})$ and $R(\theta^{(i)})$ are the approximate gradient matrix and hessian matrix of $V_N(\theta^{(i)}Z^N)$ with respect to $\theta^{(i)}$ respectively.

Also an investigation into the modeling and control of the low speed of an air motor incorporating a pneumatic equivalent of the electric H-bridge was presented by (Marumo and Tokhi, 2004). The pneumatic H-bridge had been devised for speed and direction control of the motor. The system was divided into three main regions of low, medium and high speed. The system was highly nonlinear in the low speed region and hence a controller with an ability of intelligence such as a neuro model and controller was proposed. This is the most common form of supervised learning, giving the neural networks off-line data of the plant and mapping the correlation between inputs and outputs, forming a black-box model of the plant shown in Figure (5). In the air motor neural model structure, the module, which computes pneumatic speed, is a nonlinear network, with ten sigmoidal hidden neurons and one linear output neuron. The entire control of the air motor system is achieved by the use of modular control approach cascade modeling. The modular approach opens the way to modeling of more complex behaviors of the air motor. Each module can be considered as a separate process in the input-output form:

$$Y_p(k) = f(Y_p(k-1), \dots, Y_p(k-n), U(k-1), \dots, U(k-m)) \tag{30}$$

where $Y_p(k)$ is the output vector and $U(k)$ is the input vector at time k . The goal of the modeling procedure is to build a neuro-model (NM) which predicts the process output $Y_p(k)$ as accurately as possible, given the past inputs and outputs.

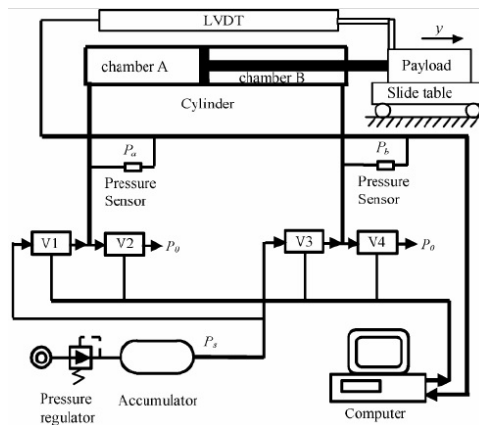


Fig. 3: Four-valves pneumatic system structure.

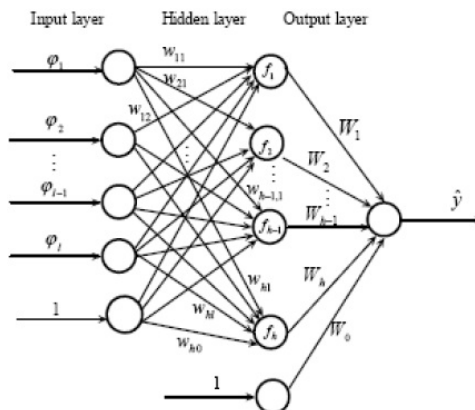


Fig. 4: A multilayered feedforward neural network.

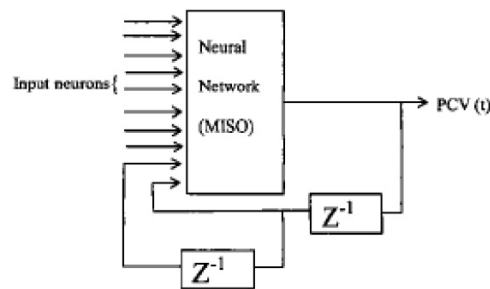


Fig. 5: Schematic of black box MISO model for pneumatic actuator system.

Conclusion:

The pneumatic actuators represent the main force control operator in many industrial applications and offer numerous advantages such as cleanliness, low cost, high ratio of power to weight, easy to maintain, safe, long anti explosion, working life and working overload. But on the other hand, the control accuracy is affected badly by its nonlinear characteristics. The nonlinear characteristics, especially the nonlinear friction and the thermodynamics of the air pressure in the chambers of the cylinder have a bad influence on control accuracy of the displacement controlling of the cylinder. In addition, there are a series of nonlinear and time varying factors such as load force, temperature, position of the piston, staying time at still and wearing out during working procedure. Also the pneumatic actuators are uncertain systems. So, because of all the reasons above, it has become necessary to find a model that can represent the actual overall dynamic behavior of the pneumatic system.

In this paper a different methodologies for deriving and simulating the model of the pneumatic actuators controlled with proportional valves are presented. The model includes cylinder dynamics, payload motion and valve characteristics. Also the intelligent methods that were used for modeling the pneumatic actuators are discussed.

REFERENCES

Armstrong, B. and C. Canudas de Wit, 1996. Friction modeling and compensation, *The Control Handbook* (by William S. Levine), CRC Press, 1369-1382.

Clements and Len., 1985. Electro-pneumatic positioners get electronics, *Journal of control and Instrumentation*, 17: 54-56.

Chen, Y.Y., J. Wang. and Q.H. Wu, 2003. A software tool development for pneumatic actuator system simulation and design, *Computers in industry*, 51: 73-88.

Djordje, D. and N. Novak, 2008. Simulation, animation and program support for a high performance pneumatic force actuator system, *Mathematical and Computer Modelling*.

Edmod, R. and H. Yildirim, 2001. A high performance pneumatic force actuator system, *ASME, Journal of Dynamic Systems, Measurement and Control*, 122(3): 4 16-425.

French, L.G. and C.S. Cox, 1988. The robust control of a modern electropneumatic actuator, *IFAC, Automatic Control In Space*.

Gary, M.B. and N. Shu, 2007. Experimental comparison of position tracking control algorithms for pneumatic cylinder actuators, *IEEE/ASME Transactions on Mechatronics*, 12(5): 557-561.

Han, K.L., S.C. Gi. and H.C. Gi, 2002. A study on tracking position control of pneumatic actuators, *Mechatronics*, 12: 813-831.

Jihong, W., K. Ulle and K. Jia, 2007. Tracking control of nonlinear pneumatic actuator systems using static state feedback linearization of the input-output map, *Proceedings Estonian Academic Science of Physics and Mathematics*, 56: 47-66.

Mark, K. and S. Nariman, 2006. QFT synthesis of a position controller for a pneumatic actuator in the presence of worst-case persistent disturbances, *Proceedings of the American Control Conference, Minneapolis, Minnesota, USA.*, 3158-3 163.

Marumo, R. and O.M. Tokhi, 2004. Intelligent modeling and control of a pneumatic motor, *CCECE, IEEE*.

Nieto, A.J., A.L. Morales, A. Gonzalez, J.M. Chicharro. and P. Pintado, 2008. An analytical model of pneumatic suspensions based on an experimental characterization, *Journal of Sound and Vibration*, 313: 290-307.

Qiang, S. and L. Fang, 2006. Neural network modeling and disturbance observer based control of a pneumatic system, IEEE.

Shu, N. and M.B. Gary, 2005. Development of a nonlinear dynamic model for a servo pneumatic positioning system, Proceedings of the IEEE International Conference on Mechatronics and Automation, Niagara falls, Canada, 43-48.

Sorli, M., L. Gastaldi, E. Codina. and S. Heras, 1999. Dynamic analysis of pneumatic actuators, Simulation Practice and Theory, 7: 589-602.

Tablin, L.B. and A.J. Gregory, 1963. Rotary pneumatic actuators, Journal of Control Engineering, 58-63.

Xuesong, W. and P. Guangzheng, 2003. Modeling and control for pneumatic manipulator based on dynamic neural network, IEEE, 223: 1-2236.

Xue, S.W., H.C. Yu. and Z.P. Guang, 2007. Modeling and self-tuning pressure regulator design for pneumatic-pressure-load systems, Control Engineering Practice, 15: 1161-1168.

Zhihong, R. and B. Gary, 2008. Nonlinear modeling and control of servo pneumatic actuators, IEEE Transactions on Control Systems Technology, 16(3): 562-569.